





Development of an osteosarcoma model with *MYCN* amplification and *TP53* mutation in hiPS cell-derived neural crest cells

Kyosuke Mukae¹  | Hisanori Takenobu¹ | Yuki Endo^{1,2}  | Masayuki Haruta¹ | Tianyuan Shi^{1,3} | Shunpei Satoh¹ | Miki Ohira¹  | Michinori Funato⁴ | Junya Toguchida⁵ | Kenji Osafune⁶ | Tatsutoshi Nakahata⁷ | Hiroaki Kanda⁸ | Takehiko Kamijo^{1,3} 

¹Research Institute for Clinical Oncology, Saitama Cancer Center, Saitama, Japan

²Department of Pediatric Surgery, Graduate School of Medicine, Tohoku University, Miyagi, Japan

³Laboratory of Tumor Molecular Biology, Department of Graduate School of Science and Engineering, Saitama University, Saitama, Japan

⁴Department of Clinical Research, National Hospital Organization, Nagara Medical Center, Gifu, Japan

⁵Department of Fundamental Cell Technology, Center for iPS Cell Research and Application, Kyoto University, Kyoto, Japan

⁶Department of Cell Growth and Differentiation, Center for iPS Cell Research and Application, Kyoto University, Kyoto, Japan

⁷Central Institute for Experimental Animals, Kanagawa, Japan

⁸Department of Pathology, Saitama Cancer Center, Saitama, Japan

Correspondence

Takehiko Kamijo, Research Institute for Clinical Oncology, Saitama Cancer Center, 818 Komuro, Ina, Saitama 362-0806, Japan.

Email: tkamijo@saitama-pho.jp

Abstract

Mesenchymal stem cell- or osteoblast-derived osteosarcoma is the most common malignant bone tumor. Its highly metastatic malignant phenotypes, which are often associated with a poor prognosis, have been correlated with the modulation of TP53- and cell-cycle-related pathways. MYC, which regulates the transcription of cell-cycle modulating genes, is used as a representative prognostic marker for osteosarcoma. Another member of the MYC oncoprotein family, MYCN, is highly expressed in a subset of osteosarcoma, however its roles in osteosarcoma have not been fully elucidated. Here, we attempted to create an in vitro tumorigenesis model using hiPSC-derived neural crest cells, which are precursors of mesenchymal stem cells, by overexpressing MYCN on a heterozygous *TP53* hotspot mutation (c.733G>A; p.G245S) background. MYCN-expressing *TP53* mutated transformed clones were isolated by soft agar colony formation, and administered subcutaneously into the perirenal adipose tissue of immunodeficient mice, resulting in the development of chondroblastic osteosarcoma. MYCN suppression decreased the proliferation of MYCN-induced osteosarcoma cells, suggesting MYCN as a potential target for a subset of osteosarcoma treatment. Further, comprehensive analysis of gene expression and exome sequencing of MYCN-induced clones indicated osteosarcoma-specific molecular features, such as the activation of TGF- β signaling and DNA copy number amplification of *GLI1*. The model of MYCN-expressing chondroblastic osteosarcoma was developed from hiPSC-derived neural crest cells, providing a useful tool for the development of new tumor models using hiPSC-derived progenitor cells with gene modifications and in vitro transformation.

Abbreviations: cNCCs, cranial NCCs; CNVs, copy number variants; DAVID, Database for Annotation, Visualization, and Integrated Discovery; GSEA, gene set enrichment analysis; hiPSCs, human induced pluripotent stem cells; InDels, insertions/deletions; KEGG, Kyoto Encyclopedia of Genes and Genomes; LF, Li-Fraumeni; MSCs, mesenchymal stem cells; MYC, MYC proto-oncogene bHLH transcription factor; MYCN, MYCN proto-oncogene, bHLH transcription factor; NCCs, neural crest cells; RP, replacement; SNVs, single nucleotide variants; TF, transformed; tNCCs, trunk NCCs.

This is an open access article under the terms of the [Creative Commons Attribution-NonCommercial-NoDerivs](https://creativecommons.org/licenses/by-nc-nd/4.0/) License, which permits use and distribution in any medium, provided the original work is properly cited, the use is non-commercial and no modifications or adaptations are made.

© 2023 The Authors. *Cancer Science* published by John Wiley & Sons Australia, Ltd on behalf of Japanese Cancer Association.

Funding information

Japan Society for the Promotion of Science, Grant/Award Number: JP 19H03625, JP 19K16759 and JP 22H04922

KEYWORDS

human induced pluripotent stem cell, MYCN proto-oncogene, neural crest cell, osteosarcoma, tumorigenesis

1 | INTRODUCTION

Many cancer studies have investigated the genetic and pharmacological actions on the mechanisms of tumor growth and cell death in tumor cells by comparing gene expression profiles between tumor and nontumor cells. However, conventional methods make it difficult to provide a complete understanding of the physiological mechanisms of tumorigenesis. Recent studies have shown the generation of sarcoma and neuroblastoma from hiPSCs. For instance, induction of *EWS-FLI1* oncogenic fusion transcript in sarcoma hiPSCs-derived osteogenic cells led to the generation of a sarcoma.¹ In addition, the administration of human hiPSCs-derived NCCs introducing neuroblastoma-specific alternations into early mouse embryos resulted in the successful generation of a neuroblastoma.² The use of hiPSC-derived tumor cells allows the tracking of temporal changes and facilitates animal tumorigenic experiments, thus making them useful for examining the efficacy of therapeutic drugs. In this study, we aimed to spontaneously induce tumorigenesis due to the introduction of an oncogene and genetic changes in genetically transformed differentiated cells.

Neural crest cells, progenitor cells of MSCs, have been efficiently differentiated from hiPSCs.³ Moreover, NCCs are multipotent cells that are mainly divided into two subgroups, cNCCs and tNCCs. cNCCs differentiate into bone and cartilage, whereas tNCCs differentiate into sympathetic ganglia and melanocytes.⁴ NCCs are of particular interest in cancer research as they constitute the origin of various tumors, including small-cell lung cancer, osteosarcoma, neuroblastoma, and glioblastoma.⁵ MYC is involved in the process of differentiation of NCCs into osteoblasts, while MYCN is involved in the process of differentiation of NCCs into sympathetic ganglia; consistently, hyperregulation of these processes is considered to lead to tumorigenesis.^{6,7} The MYC family members, MYC and MYCN, are representative oncogenes and have been widely used to generate mouse models of cancer, such as breast cancer and neuroblastoma.^{8,9}

Using an established cNCC differentiation protocol, we induced the generation of cNCCs from WT hiPSCs and LF syndrome patient-derived hiPSCs, and subsequently introduced MYCN into these cNCCs using lentiviral transfection to study the MYCN-related oncogenic mechanism in the hiPSC-derived cNCCs.³ Transfected NCCs were cultured in soft agar medium and TF clones were isolated. We administered these LF-derived/MYCN-transduced TF clones both subcutaneously and into the perirenal adipose tissue of immunodeficient mice, resulting in the generation of high-grade chondroblastic osteosarcoma. Here, we investigated the molecular features of tumorigenesis of this high-grade osteosarcoma using comprehensive gene expression and whole-exome analyses compared with previous reports on osteosarcoma.

2 | METHODS AND MATERIALS

Expanded methods can be found in Appendix S1.

2.1 | Pluripotent stem cell maintenance

The 414C2 and LF human iPSC lines were provided by Dr. Kenji Osafune (Kyoto University, Kyoto, Japan). LF hiPSCs carry a heterozygous *TP53* hotspot mutation (c.733G>A; p.G245S). Both cell lines were maintained on a feeder layer of mitomycin C-treated embryonic mouse fibroblasts in primate embryonic stem (ES) cell medium (REPROCELL, Tokyo, Japan) supplemented with 4 ng/mL recombinant human FGF2 (FUJIFILM, Tokyo, Japan). The 414C2 hiPSC cell line was generated from a healthy person.¹⁰ The LF hiPSC cell line was generated by transducing episomal vectors (OCT3/4, SOX2, KLF4, L-MYC, LIN28, and p53shRNA) in dermal fibroblasts from a patient with LF syndrome.

3 | RESULTS

3.1 | Differentiation of 414C2 and LF hiPSCs into cNCCs and preparation of MYCN-overexpressing cells

We subjected 414C2 and LF hiPSCs to differentiation into cNCCs according to the reported protocol.³ Using the neurotrophin receptor (p75, a cell surface marker of NCCs), we collected the p75-positive cells by cell sorting (Figure S1). We then subjected the sorted cNCCs to gene expression analysis of stem cell and NCC markers (Figure 1A). We found that the sorted cNCCs expressed representative markers of NCCs, such as *PAX3*, *p75*, *SOX10*, and *ETS1*.³ In contrast, we detected that the expression of *OCT4* was clearly downregulated in cNCCs compared with that in hiPSCs. We infected these cNCCs with either control (mock) or MYCN-expressing (MYCN) lentiviruses. Subsequently, we analyzed the infected cNCCs by RT-PCR and western blotting to confirm the induction of the gene and protein expression of MYCN. Notably, we observed that the expression of MYCN was increased in LF-derived cNCCs compared with that in 414C2-derived cNCCs (Figure 1B,C).

3.2 | Transformation using the soft agar colony formation assay

We performed the soft agar colony formation assay using mock- or MYCN-expressing 414C2- and LF cNCCs. We found that for 414C2

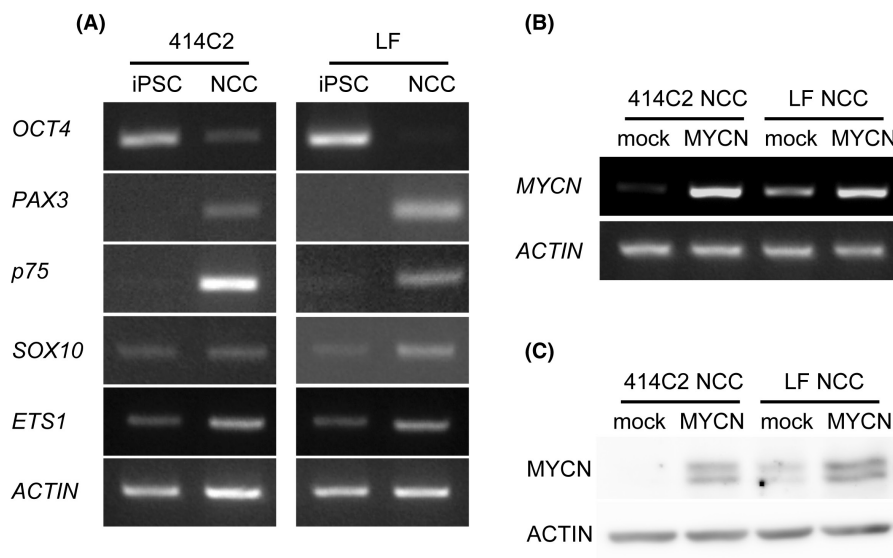


FIGURE 1 Expression profiles of cNCCs differentiated from hiPSCs and preparation of MYCN-overexpressing cNCCs. (A) Semiquantitative RT-PCR analysis of the expression of pluripotency (*OCT4*) and neural crest (*PAX3*, *p75*, *SOX10*, and *ETS1*) markers in 414C2, LF hiPSCs, and cNCCs. Primers used were specific for transcripts from the respective endogenous locus. *ACTIN* was used as a loading control. (B, C) 414C2 and LF cNCCs were infected with control (mock) or MYCN-expressing (MYCN) lentivirus. Infected cells were analyzed for expression of the gene and protein of MYCN.

cNCCs, MYCN-expressing cells formed more colonies than mock-transduced cells. However, LF cNCCs formed many colonies regardless of MYCN transduction, suggesting that the elevated levels of MYCN in LF NCCs caused anchorage-independent proliferation (Figures 1C and 2A). We isolated the clones from four 414C2 mock, 20 414C2 MYCN, 17 LF mock, and 23 LF MYCN colonies (Figure 2B). We cultured these clones in complete CDMi medium-containing culture plates, and successfully established 20 414C2 MYCN, 11 LF mock, and 14 LF MYCN clones. We confirmed the level of expression of MYCN in the selected clones by western blotting and RT-PCR, and found that MYCN-transduced clones had higher levels of expression of MYCN compared with that in mock cNCCs (Figure 2C: upper panel). Additionally, the selected clones showed a higher capacity for colony formation than either mock- or MYCN-transduced cNCC (Figure 2C: lower panel).

3.3 | Tumorigenesis experiments by subcutaneous administration

We selected the well-grown clones (Figure 2C: upper panel) and subcutaneously administered 414C2 (MYCN TF-1 to TF-3) and LF (mock TF-1 to TF-3 and MYCN TF-1 to TF-4) cNCC clones to BALB/c Ajcl nu/nu mice. We observed that 414C2 MYCN TF clones did not generate any tumor masses (three out of three). However, we detected the generation of tumor masses in two out of four LF mock TF-3, one out of four LF MYCN TF-1, and two out of four LF MYCN TF-4 clones (Figure 3A). In contrast, LF mock TF-1, and -2, as well as LF MYCN TF-2 and -3 did not generate any tumor masses. We found the apparent development of bone and cartilage with atypical spindle cells in all masses and identified all generated tumors as chondroblastic osteosarcoma according to

H&E staining (Figure 3B). PCNA (proliferation marker) immunostaining showed cell proliferation in all masses (Figure 3B). We also detected a high PCNA labeling index (98.3%) in the tumor derived from LF MYCN TF-4 (Figure 3C). According to the percentage of PCNA, we defined more than 70% as high grade (LF MYCN TF-4), between 30% and 70% as intermediate, and less than 30% as low grade. In addition, to examine the effects of tumorigenesis in TP53 and MYCN, lentivirus-infected mock- or MYCN-expressing 414C2- and LF cNCCs were administered subcutaneously to SCID/Beige mice, which are more severely immunodeficient than BALB/c Ajcl nu/nu mice. We found that LF mock- and LF MYCN-expressing cNCCs generated masses that were larger than the 414C2 mock- and 414C2 MYCN-expressing cNCC masses, respectively, suggesting a positive effect of the TP53 mutation on osteosarcoma tumorigenesis (Figures S3 and S4). H&E staining showed that all tumor sections contained bone tissues, which were assumed to be due to differentiation into cNCCs (Figure 3D). Also, the mutation of TP53 and expression of MYCN induced the formation of nuclear atypia (H&E; Figure 3B,D) and increased the PCNA expression in LF MYCN-expressing clones (PCNA, Figure 3B,D). These results indicated that the co-occurrence of overexpression of MYCN with TP53 mutation and transformation by anchorage-independent proliferation induced high-grade tumorigenesis.

3.4 | Tumorigenesis experiments by administration of transformed clones into the perirenal adipose tissue of mice

NCCs are embryonic precursor cells that are involved in the development of multiple pediatric malignancies, including neuroblastoma, peripheral primitive neuroectodermal tumors, and

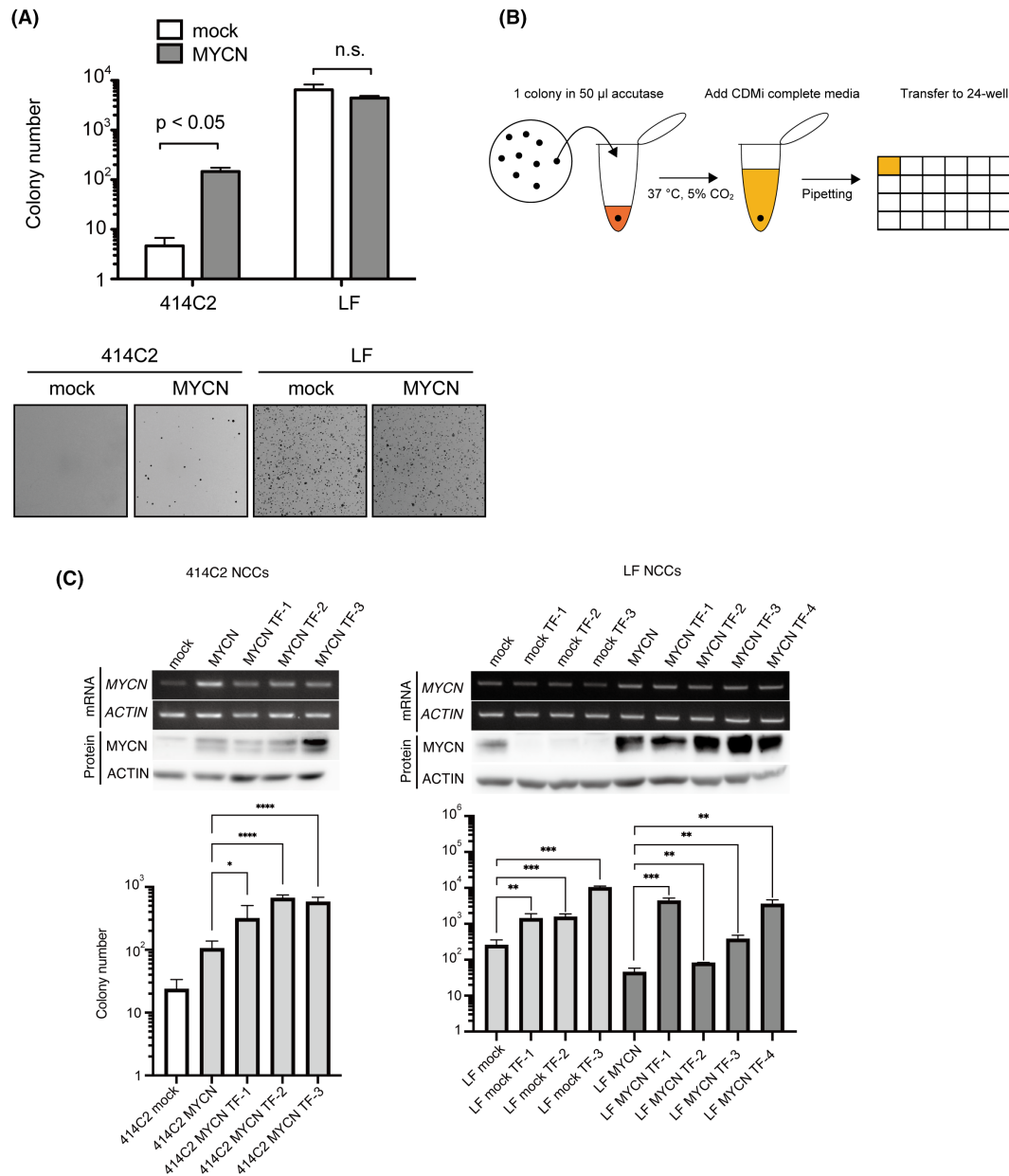


FIGURE 2 Isolation of transformed cells using the soft agar colony formation assay. (A) Anchorage-independent growth ability was evaluated by soft agar colony formation assay. Colonies were counted using the Clono-Counter software. Results were represented as the mean \pm SD of triplicate samples. (B) Protocol for the isolation of colonies from soft agar dishes. A single colony was isolated in a 1.5 mL tube containing 50 μ L accutase and pipetted with CDMi medium. Pipetted clones were cultured in 24-well plates. (C) Western blotting and semiquantitative RT-PCR analysis (upper panel) of the expression of MYCN in isolated 414C2 MYCN TF 1–3, LF mock TF 1–4, and LF MYCN TF 1–4 clones. ACTIN was used as loading control. The lower panel shows anchorage-independent growth ability evaluated by soft agar colony formation assay. Results are represented as the mean \pm SD of four replicates.

osteosarcoma.^{11,12} To investigate the tumorigenic ability of the tumor-generated TF clones (Figure 3) when implanted into mice that are more immunodeficient compared with BALB/c Ajcl nu/nu mice, we implanted LF mock and MYCN-expressing cNCCs, and TF clones into the perirenal adipose tissue of SCID/Beige mice. We observed that all generated masses contained bone tissues. Although only one out of five LF mock TF-3 led to the generation of tumors, we detected 100% tumor generation by LF MYCN TF-1,

TF-4 clones, and LF MYCN-expressing cNCCs (Tables 1 and 2). We specifically identified these generated tumors as chondroblastic osteosarcoma and designated them: LF MYCN CO-1 (generated by LF MYCN cNCCs), LF MYCN CO-2 (generated by LF MYCN TF-1), and LF MYCN CO-3 (generated by LF MYCN TF-4) (Figure 4A). The H&E staining showed a higher tumor cell density, more prominent cell division, and higher necrosis in LF MYCN CO-3 compared with LF MYCN CO-2 (Figure 4A). We further observed that all

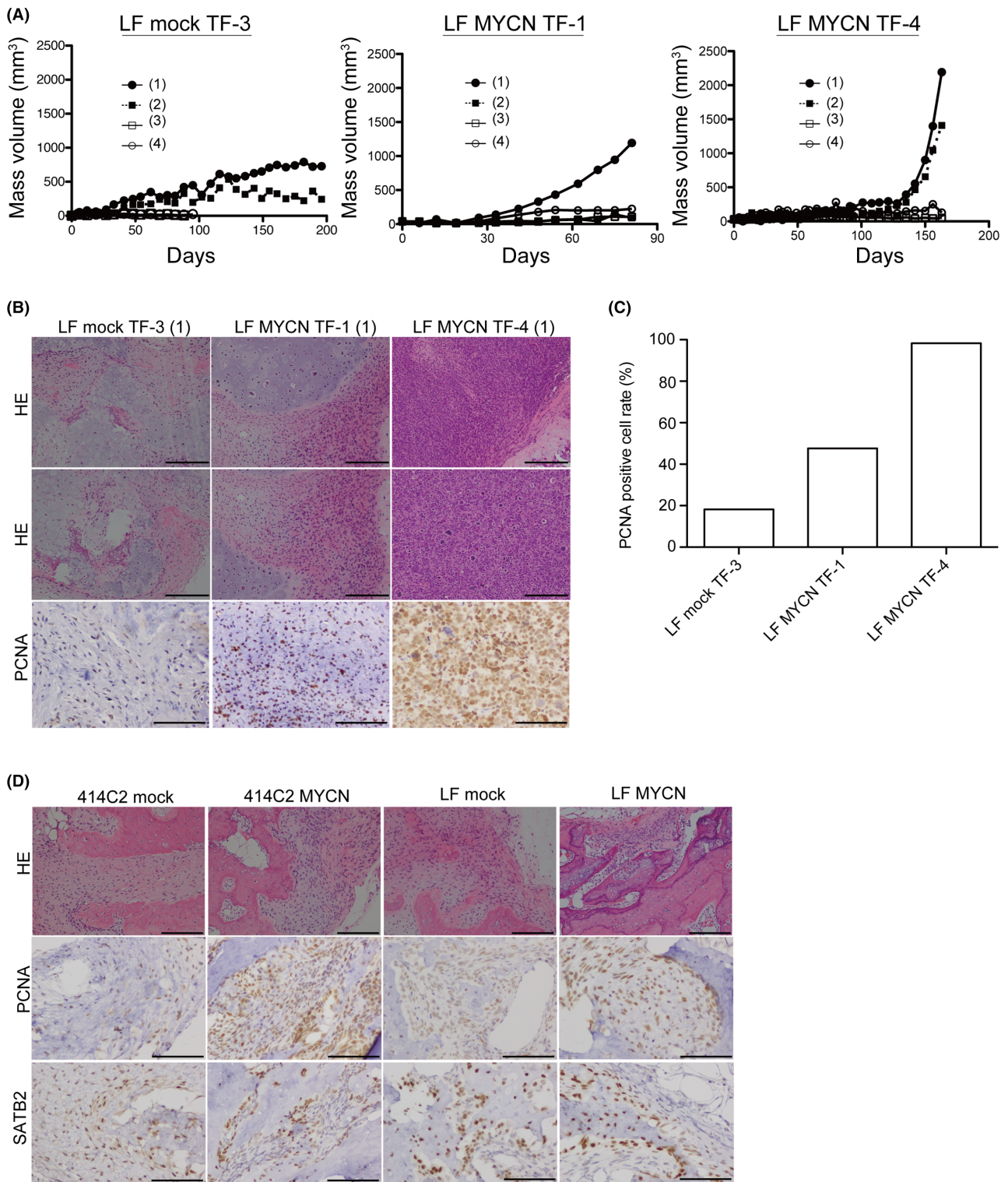


FIGURE 3 Subcutaneous administration with mock and MYCN cNCCs/TF clones of 414C2 and LF into BALB/c AJcl-nu/nu mice. (A) BALB/c AJcl-nu/nu mice were subjected to subcutaneous xenografts using 414C2 MYCN, LF mock, or LF MYCN TF clones. Respective TF clones were administered to four independent parts, as described in Methods. Proliferating TF clones are shown. Mice whose tumor mass volume did not reach 50mm^3 after 3 months were not included. (B) H&E staining from regions with bone and chondroblastic osteosarcoma of generated masses in LF mock TF-3 (1), LF MYCN TF-1 (1), and LF MYCN TF-4 (1). Scale bars: $200\mu\text{m}$. Tissue samples were analyzed immunohistochemically for PCNA-positive cells. Scale bars: $200\mu\text{m}$. (C) Quantitation of PCNA-positive cells in LF mock TF-3 (1), LF MYCN TF-1 (1), and LF MYCN TF-4 (1) by counting >1000 tumor cells. (D) H&E staining from regions with bone and chondroblastic osteosarcoma of generated masses in lentiviral-infected mock and MYCN cNCCs of 414C2 and LF cells. Scale bars: $200\mu\text{m}$. Tissue samples were analyzed immunohistochemically for PCNA- and SATB2-positive cells. Scale bars: $200\mu\text{m}$.

TABLE 1 Incidence of tumorigenesis in mice administered with cNCCs or transformed clones into the periadrenal adipose tissue.

Clone name	Number of tumor mass/injected mice
414C2 MYCN TF-1	0/2
LF mock NCCs	0/4
LF mock TF-3	1/5
LF MYCN NCCs	3/3
LF MYCN TF-1	3/3
LF MYCN TF-4	2/2

TABLE 2 Tumor sizes and the periods of tumorigenesis related to Table.

Line	Size (mm ³)	Period (days)
LF Mock TF-3 (LF Mock CO)	84.91	259
LF MYCN (LF MYCN CO-1)	564.93	235
LF MYCN	84.79	291
LF MYCN	ND	117
LF MYCN TF-1 (LF MYCN CO-2)	158.16	120
LF MYCN TF-1	77.58	228
LF MYCN TF-1	ND	359
LF MYCN TF-4	8.38	118
LF MYCN TF-4 (LF MYCN CO-3)	4203.00	198

Abbreviation: ND, not detected due to post-freezing.

histologically assessed tumors were positive for PCNA and SATB2 (a marker for osteoblastic differentiation), with LF MYCN CO-1 being intermediate; CO-3 tumors were high grade, and LF MYCN CO-2 tumor were low grade. Interestingly, the LF mock CO tumor was an intermediate tumor of chondroblastic osteosarcoma generated by LF mock TF-3 (Figure 4A,B). We analyzed the osteosarcoma-related gene (*BMI1*, *GAL-1*, *EZR*, and *RUNX2*) expression in LF mock- and LF MYCN-expressing cNCCs, LF mock TF-3, LF MYCN TF-1, and LF MYCN TF-4 clones, as well as in LF mock CO/LF MYCN CO-1, -2, and -3 tumors (Figure 4C). In particular, we detected that tumorigenesis further increased the expression of MYCN compared with that in the administered clones. We found that the levels of osteosarcoma-related genes were upregulated in LF MYCN CO-1, -2, and -3, and in LF mock CO tumors, indicating that all generated tissues had genetic features of osteoblasts or osteosarcoma, including chondroblastic osteosarcoma. In addition, we detected that *RUNX2* and its downstream genes (*FGFR2*, *FGFR3*, *SP7*, and *SMOC2*) were downregulated in the highly aggressive LF MYCN CO-3 clone (Figure 4C). *RUNX2* is reported to regulate osteoblast differentiation^{13,14} and suppress osteosarcoma cell proliferation.¹⁵ We also found that LF MYCN CO-3 had the same PCNA rate as LF MYCN CO-1, but exhibited higher grade features in terms of H&E staining and lower expression of *RUNX2*, suggesting the tumor suppressor function of *RUNX2* in cNCC-derived chondroblastic osteosarcomas.

3.5 | Genetic changes during the transition from cNCCs to tumorigenic clones

To uncover the mechanisms underlying tumorigenesis, we performed gene expression profiling using microarray analyses of LF mock cNCCs, LF MYCN cNCCs, LF MYCN TF-4 clones, and LF MYCN CO-3 tumors. Our principal component analysis separated distinctly the four different groups of samples (Figure 5A). Previous studies have reported the activation of pathways such as TGF- β , NF-kappa B, and WNT signaling in osteosarcoma.^{16,17} Therefore, we analyzed the upregulated genes (moderated *t*-test of <0.01 and fold changes of >2) using the KEGG pathway analysis program from DAVID v6.8. Functional annotation of upregulated genes suggested that the NF-kappa B signaling pathway, basal cell carcinoma, TGF- β signaling pathway, and cytokine-cytokine receptor interaction were significantly enriched in the process of tumorigenesis (Figure 5B). Subsequently, among these pathways, we focused on the genes in the TGF- β signaling pathway and basal cell carcinoma, including bone morphogenetic proteins, and compared the expression of representative genes among cells, clones, and tumors using RT-PCR (Figure 5C). We found that LF MYCN CO-3 showed significantly higher expression of genes involved in the TGF- β signaling pathway affecting osteosarcoma tumor growth and basal cell carcinoma, suggesting the increased expression of cell proliferation-related genes during the process of transition to becoming a high-grade tumor (Figure 5C; Table S1). In addition, GSEA suggested that LF MYCN CO-3 displayed tumor characteristics that were more associated with MSC-derived sarcomas obtained from soft tissue and bone compared with LF mock cNCCs (Figure 5D).¹⁸⁻²² These results indicated that LF MYCN CO-3 exhibited features characteristic of osteosarcoma, as indicated in Figures 4 and 5.

3.6 | Suppression of MYCN in osteosarcoma cell lines

Although the malignant phenotypes of osteosarcoma are known to be related to the high expression of c-MYC, little has been reported on the relationship between MYCN and osteosarcoma.²³ Interestingly, the expression of MYCN has been shown to be higher in osteosarcoma than that in MSC and this higher expression has been related to a lower overall survival probability in osteosarcoma (Figure S2). To investigate the level of expression of MYCN in osteosarcoma cell lines, we analyzed the expression of both MYC and MYCN in Saos-2, SJSA-1, NY, and G-292 cells. As SJSA-1 and NY expressed low levels of MYCN (Figure 6A,B), we knocked down MYCN in these two osteosarcoma cell lines using two types of shRNA (shMYCN2 and shMYCN3). After infection, we assessed the expression of MYCN using RT-PCR and western blotting, and found that the levels of both MYCN mRNA (Figure 6C,D: upper panel) and protein were decreased by either of the shMYCNs (Figure 6C,D: middle panel). We further performed a viability assay of the infected cell lines and found that shMYCNs clearly suppressed the proliferation of SJSA-1 and NY (Figure 6C,D: lower panel).

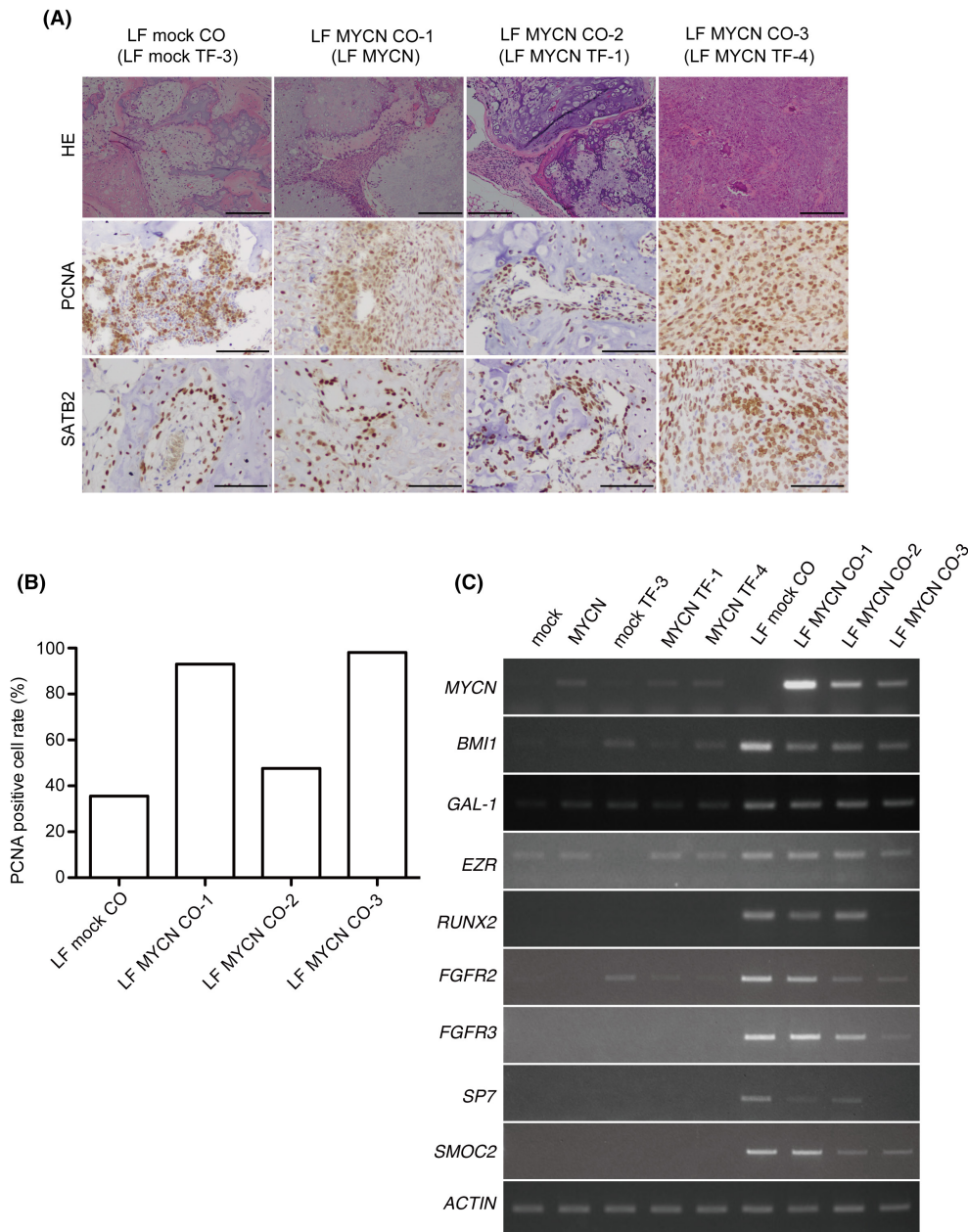


FIGURE 4 Tumorigenesis experiments by administration of transformed clones into the periadrenal adipose tissue of SCID/Beige mice. (A) Indicated cell lines in Matrigel® were administered into the periadrenal adipose tissue of mice. H&E staining of bone and chondroblastic osteosarcoma developed from LF mock CO (LF mock TF-3), LF MYCN CO-1 (LF MYCN cNCCs), LF MYCN CO-2 (LF MYCN TF-1), and LF MYCN CO-3 (LF MYCN TF-4) are shown. Scale bars: 200 μ m. Tissue samples were analyzed immunohistochemically for PCNA- and SATB2-positive cells. Scale bars: 200 μ m. (B) Quantitation of PCNA-positive cells in LF mock CO, LF MYCN CO-1, CO-2, and CO-3 by counting >1000 tumor cells. (C) Semiquantitative RT-PCR analyses of the expression of *MYCN*, *BMI1*, *GAL-1*, *EZR*, and *RUNX2* among LF-infected cNCCs, TF clones, and COs samples. *ACTIN* was used as loading control.

3.7 | Analysis of genomic changes using whole-exome sequencing

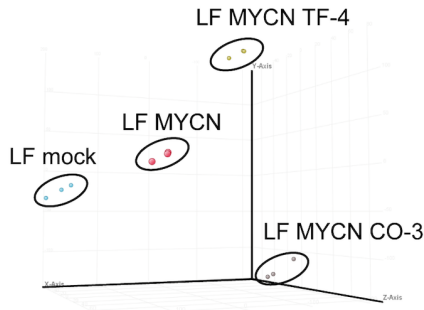
Although both LF MYCN CO-2 and CO-3 tumors had a molecular background of *TP53* mutation and overexpression of *MYCN*, compared with LF MYCN CO-2, LF MYCN CO-3 showed a higher grade tumor phenotype, as revealed from pathological analysis (Figures 3B and 4A). To address this difference, we performed whole-exome

sequencing of LF hiPSC, LF MYCN CO-2, and CO-3. Whole-exome sequencing of LF MYCN CO-2 and CO-3 revealed the presence of SNVs, RP, and InDels on LF hiPSCs as the reference, and mutations that were only found in LF MYCN CO-3, as shown in Table S2. Among the 29 extracted mutations collated using dbSNP and ClinVar, we detected three mutations in *AQP7*, *DYX1C1*, and *NOL12*, which mutations are reported as benign or unknown (Table S2). Annotation was performed for the pathogenicity of all extracted mutations using

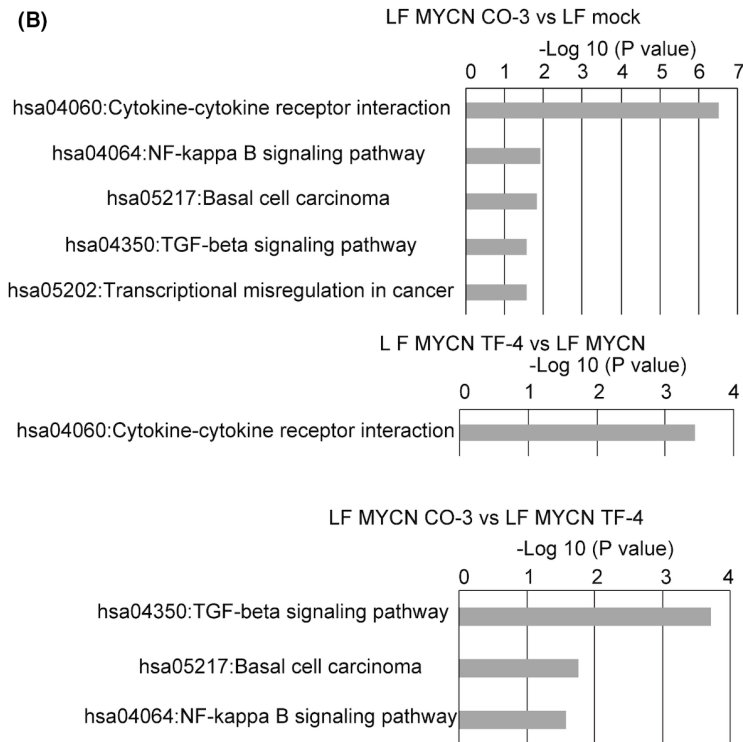
specific prediction tools (FATHMM CScape for SNVs and PredCID for RP and indels) to analyze the mutations in LF MYCN CO-3 related to high-grade phenotypes. FATHMM CScape showed high-confidence

predictions for oncogenic mutations in *USP2*, *POTEM*, and *DYX1C1*. PredCID predicted driver mutations in *MAP3K1* and *AR*, specifically stop-gain mutations (Figures S5 and S6).

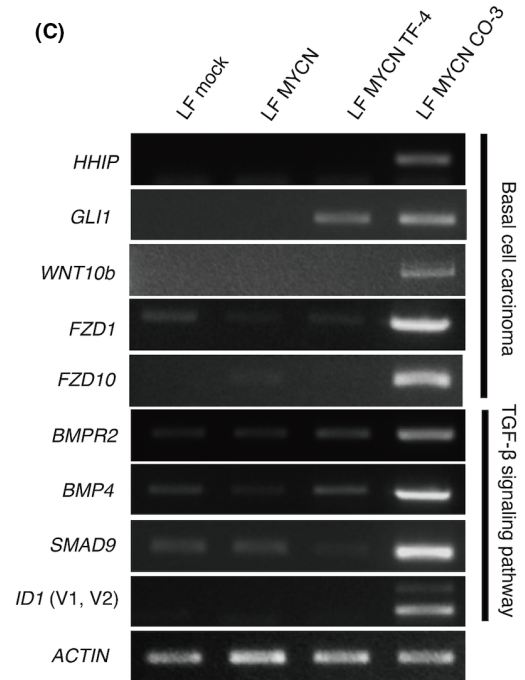
(A)



(B)



(C)



(D)

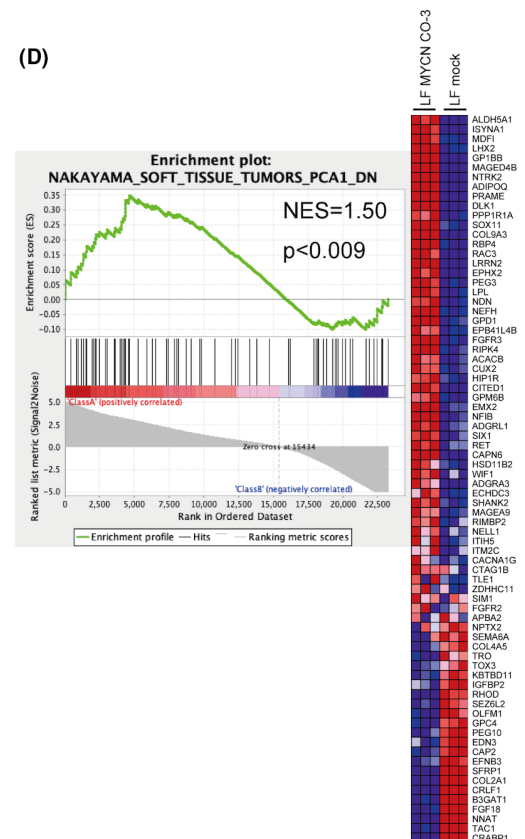


FIGURE 5 Microarray analysis of the process of tumorigenesis. (A) 3D principal component analysis showed variations in gene expression among LF mock cNCCs ($n = 3$), LF MYCN cNCCs ($n = 3$), LF MYCN TF-4 ($n = 3$), and LF MYCN CO-3 ($n = 3$). (B) Pathway analysis using the KEGG pathway (DAVID Bioinformatics Resources 6.8) for genes upregulated more than two-fold ($p < 0.01$) in LF MYCN CO-3 compared with LF mock cNCCs, in LF MYCN TF-4 compared with LF MYCN-cNCC, and in LF MYCN CO-3 compared with LF MYCN TF-4. (C) Semiquantitative RT-PCR analyses of the expression of genes related to basal cell carcinoma (*HHIP*, *GLI1*, *WNT10b*, *FZD1*, and *FZD10*) and TGF- β signaling (*BMP2*, *BMP4*, *SMAD9*, and *ID1*) pathways in LF-infected cNCCs, LF MYCN TF-4, and LF MYCN CO-3. *ACTIN* was used as loading control. (D) Genes differentially expressed between LF MYCN CO-3 and LF mock cNCCs share molecular signatures as determined by gene set enrichment analysis (GSEA) with gene sets downstream of "NAKAYAMA_SOFT_TISSUE_TUMORS_PCA1_DN."

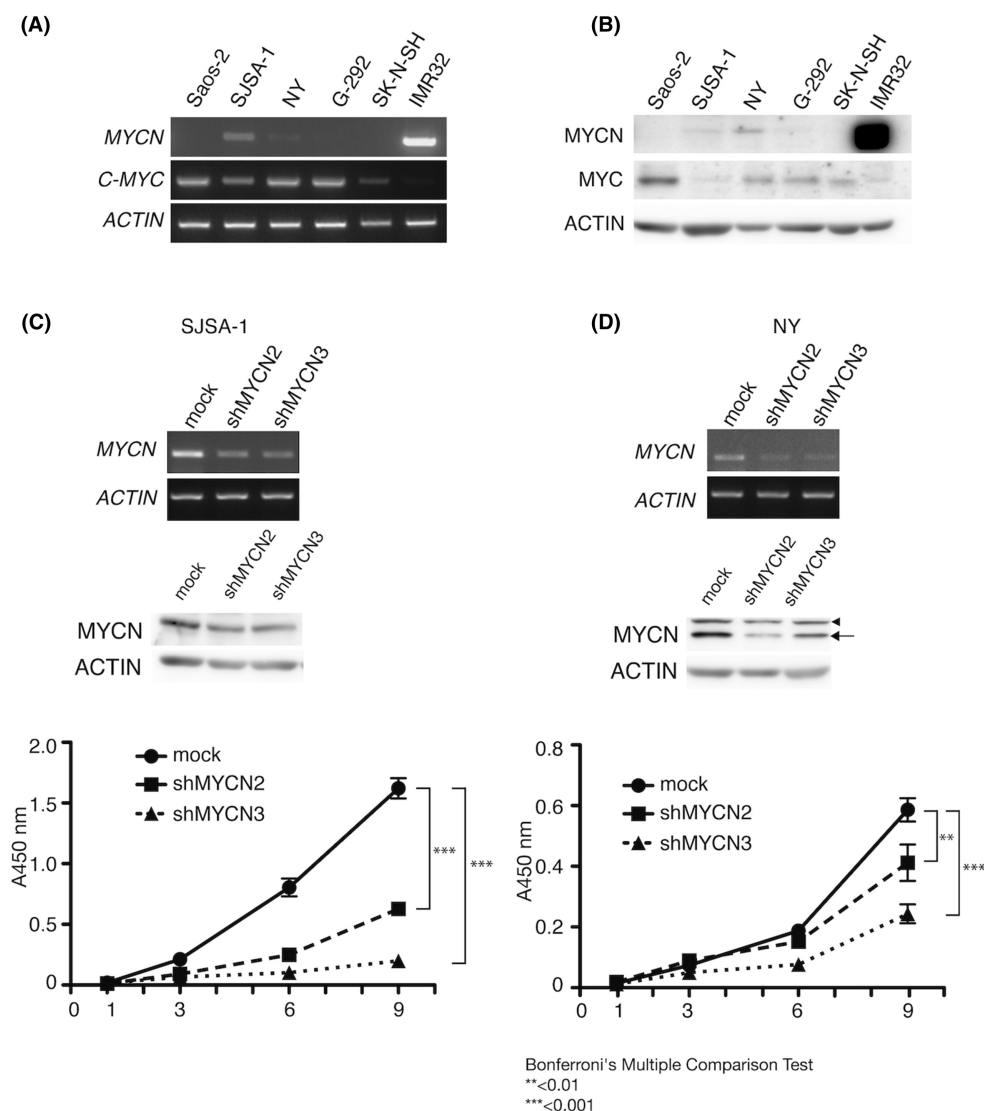
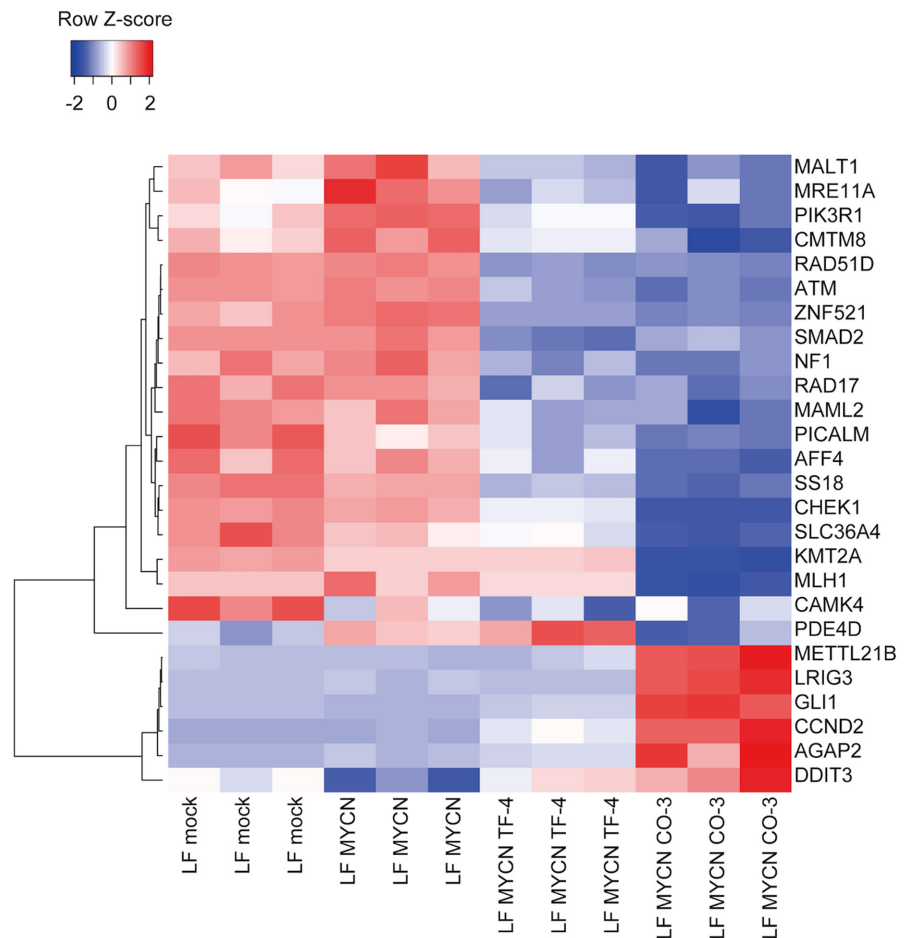


FIGURE 6 MYCN depletion in MYCN-expressing osteosarcoma cells. Semiquantitative RT-PCR (A) and western blotting (B) analyses of the expression of MYCN (MYCN) and c-MYC (MYC) in osteosarcoma (Saos-2, SJSA-1, NY, and G-292) and neuroblastoma (SK-N-SH and IMR32) cell lines. SK-N-SH was used as a negative control, whereas IMR32 was used as a positive control for the expression of MYCN. *ACTIN* (*ACTIN*) was used as a loading control. (C) SJSA-1 and (D) NY were infected with control (mock) or shMYCN-expressing lentivirus. Infected cells were analyzed for the expression of the gene (upper panel) and protein (middle panel) of MYCN. SJSA-1 and NY cells (mock, shMYCN2, and shMYCN3) were seeded on a 96-well plate at a concentration of 700 cells/well in 100 μ L culture medium. Cell proliferation was studied at the indicated time points (1, 3, 6, and 9 days) (lower panel). Bars indicate standard deviation from four replicates.

We analyzed all sequencing data for LF MYCN CO-2 and LF MYCN CO-3 with LF hiPSCs as the reference, utilizing a custom workflow in CLC Genomics Workbench version 20.0 to identify CNVs of genes detected only in LF MYCN CO-3. We found that despite no

amplifications and 74 deletions of CNVs in LF MYCN CO-2 versus LF hiPSCs, CNVs in LF MYCN CO-3 included 143 amplifications and 1855 deletions of genes versus LF hiPSCs ($p < 0.01$, fold change FC: 1.8). Homozygous deletions were not detected. Interestingly, among

FIGURE 7 Expression profiles of downregulated and upregulated genes in LF MYCN CO-3. Clustering analyses using average linkage and Pearson's correlation distance were performed for downregulated genes in focal deletions ($FC < 0.5$) and upregulated genes in focal amplifications ($FC > 2$) in LF MYCN CO-3 compared with those in LF mock or LF MYCN cNCCs.



the LF MYCN CO-3 unique genetic changes, we analyzed specific osteosarcoma-associated CNVs using previous reports^{24,25} and databases for osteosarcoma (osteosarcoma markers in the MY CANCER GENOME database), and detected 15 amplifications and 50 deletions (Table S3). Additionally, these identified genes were examined for fold changes in their downregulated ($FC < 0.5$, for a candidate tumor suppressor gene, TSG) or upregulated ($FC > 2$, for a candidate oncogene) expression in LF MYCN CO-3 compared with that in either LF mock or LF MYCN cNCCs in our microarray data (Figure 7). We accordingly identified 13 candidate TSGs and six candidate oncogenes, and especially found that GLI1 was highly upregulated in the LF MYCN CO-3 tumor (Figure 5C; Table S3).

4 | DISCUSSION

In recent years, there has been an increased interest in exploring the transformation of stem and progenitor cells in the research of tumorigenic mechanisms. Sato et al. demonstrated that in vitro transformation of human lung epithelial cells, as defined by anchorage-independent growth in soft agar, led to tumorigenesis.²⁶ Also in our study, the transformation of cNCCs by soft agar colony formation generated high-grade tumors. These previous reports and finding suggested that high-grade in vivo tumorigenicity requires

anchorage-independent transformation, accompanied by genetic mutations and epigenetic modifications. In fact, in our microarray analysis, we observed that the introduction of the MYCN alone did not result in extensive alternations in pathways, but the activation of pathways related to the generation of osteosarcoma was achieved due to transformation and tumorigenesis. These findings revealed that the introduction of a single oncogene to stem and progenitor cells seems to not be enough for the induction of tumorigenesis. In addition to oncogene transduction, additional genetic and epigenetic modifications induced by cellular stress mediated by anchorage-independent colony formation appear to be required. Previous studies of models using differentiated cells from hiPSCs achieved effective tumorigenesis following the transplantation of differentiated cells in which two or more genes had been manipulated, and showing the potential for clinical application,^{2,27,28} similar to our results in immunodeficient mice. Furthermore, in this study, the soft agar colony formation assay had the potential to promote tumorigenesis of chondroblastic osteosarcoma from cNCCs. Therefore, our study suggested that soft agar colony formation would be useful for inducing spontaneously oncogenic events in hiPSC-originated progenitor cells, thereby enabling the acquisition of the desired cancer type through the simple operation of transplantation.

It has been previously suggested that p53 dysfunction leads to osteosarcoma tumorigenesis, which has been shown in vitro

using LF hiPS cell-derived osteoblasts.²⁹ MSCs and osteoblasts are predicted as the origin of osteosarcoma,³⁰ and in this study, osteosarcoma was generated from NCCs, which is a further undifferentiated state. Amplification of MYC is frequently observed in osteosarcoma, and thus c-MYC is used as a prognostic biomarker.¹⁶ The MYC family also includes MYCN and MYCL. A previous study showed the relationship between the expression of MYCN and osteosarcoma, although it was considerably less than that of C-MYC.³¹ In our study, all generated tumors were pathologically diagnosed as chondroblastic osteosarcoma. Microarray analysis of the molecular profile revealed the activation of pathways such as cytokine–cytokine receptor interaction, NF-kappa B signaling, and TGF- β signaling, which are known to be frequently activated in osteosarcoma (Figure 5B).¹⁶ BMI1 is known to function as an oncogene in osteosarcoma, promoting tumorigenesis. Interestingly, tumorigenesis has been shown to upregulate BMI1,³² which is the same finding in the expression of MYCN in our study. In addition, the expression of GAL-1³³ and EZR,³⁴ which have been reported as chondroblastic osteosarcoma markers, was increased during tumorigenesis (Figure 4C). RUNX2 is the earliest determinant of osteoblast differentiation, and its forced expression has been shown to suppress the proliferation of osteosarcoma cell lines, suggesting that LF MYCN CO-3 is high grade compared with LF MYCN CO-1.¹⁵ Although the relationship between chondroblastic osteosarcoma and TP53 mutation is known, its relationship to MYCN status has not been reported.^{30,35} Our study showed that MYCN appears to be an indispensable molecule for the proliferation of MYCN-expressing osteosarcoma cells and is the first to identify the oncogenic roles and mutagenic effects of MYCN transduction into hiPSCs-derived cNCCs. These findings will be helpful for the functional study of mutated or modified genes in osteosarcoma. Osteosarcomas include fibroblastic, osteoblastic, and chondroblastic subtypes; the unique changes in gene expression in chondroblastic osteosarcoma include the upregulation of ACAN, a cartilage-specific proteoglycan core protein, and MATN4, a major component of the extracellular matrix of cartilage.³⁶ It hence might be possible to induce chondroblastic osteosarcoma by introducing ACAN or MATN4 using TP53-deficient cNCCs. Additionally, it might be possible to generate fibroblastic or osteoblastic osteosarcoma by introducing specific genes in osteosarcoma cells.

When we compared LF MYCN CO-2 (low-grade) and LF MYCN CO-3 (high-grade) tumors, we found that the CNV alterations were more frequent in LF MYCN CO-3. This finding indicated that CNVs in LF MYCN CO-3 might have an important role in osteosarcoma aggressiveness. Interestingly, a previous study on CNVs in osteosarcoma showed both gain and loss on multiple chromosomes in chondroblastic types.³⁷ In particular, loss of chromosome 3q, loss of chromosome 17q, and gain of chromosome 12q were also found in this study, suggesting that CNVs in these regions might be unique to chondroblastic osteosarcoma and might thus serve as diagnostic markers. In addition, we focused on six genes showing a gain on chromosome 12 and upregulation of transcription as chondroblastic

osteosarcoma oncogene candidates: *GLI1*, *DDIT3*, *CCND2*, *AGAP2*, *METTL21B*, and *LRIG3* (Figure 7; Table S3). As many studies have previously demonstrated, 12q gains and several genes on 12q have been strongly correlated with osteosarcoma malignancies. Apart from *DDIT3* and *LRIG3*, oncogenic roles have been reported for *GLI1*, *CCND2*, *AGAP2*, and *METTL21B* in several tumors.^{38–41} For instance, *GLI1* has been reported to be amplified in osteosarcoma; *GLI1* copy number was similarly amplified in LF MYCN CO-3 (Tables S3 and S4).⁴² In addition, *GLI1* inhibition by shRNA decreased colony and sphere formation in cultured osteosarcoma cells, whereas upregulation of *GLI1* has been shown in other tumor types,^{38,42} consistent with the observed upregulation of *GLI1* in LF MYCN CO-3 in our study. Hence, the CNVs of these genes might be involved in a complex manner in the development of high-grade phenotypes of LF MYCN CO-3.

Based on SNVs and CNVs studies, 11 genes were identified as candidates mediating chondroblastic osteosarcoma tumorigenesis and aggressiveness (Figure 7; Tables S2 and S3). Among them, driver gene candidates, for which inhibitors exist, were *MAP3K1*, *AR*, *USP2*, and *GLI1*. Several stop-gain mutations, such as the R183X mutation in *MAP3K1* (genomic mutation ID: COSV68128873), have been registered in the COSMIC and dbSNP databases (Figure S5). This *MAP3K1* (R183X) mutation was registered as pathogenic in the COSMIC database. Likewise, the Q59X mutation in *AR* has also been registered in the COSMIC and dbSNP databases as a stop-gain mutation (genomic mutation ID: COSV65954985) (Figure S6), while it has also been registered as pathogenic in the ClinVar database (ClinVar accession: VCV000643319.1). These driver gene candidates, shorter *MAP3K1*, and *AR* in chondroblastic osteosarcoma, might not be functional, and therefore tumor progression is expected to be blocked by inhibitors of their downstream JNK (such as tanzisertib) for *MAP3K1* or Src (such as dasatinib) for *AR*. In addition, there are *USP2* [ML364 (#S6748)] and *GLI1* [GANT61 (#S8075)] inhibitors. Although these inhibitors are now only for research use, the *USP2* and *GLI1* inhibitors have been reported to be effective against breast cancer and chondrosarcoma cells, respectively.^{43,44} In addition, although *CCND2* is not a druggable target, there are *CDK4/CDK6* inhibitors, such as palbociclib, that form a complex with *CCND2*. Adding these to the treatment options for chondroblastic osteosarcoma might lead to an improved prognosis.⁴⁵

In conclusion, we developed a model of chondroblastic osteosarcoma with high expression of MYCN using LF hiPSCs-derived cNCCs. Genetic analysis of the acquired mutations in the MYCN-transduced cNCCs, as well as transformation by soft agar colony formation and xenograft chondroblastic osteosarcoma assays, clarified the process of stepwise genetic mutations during osteosarcoma tumorigenesis (Figure 8). Although the number of clones examined in this study was limited, the pathological and genetic analyses of these clones confirmed the previous reports from osteosarcoma studies. A wide variety of tumorigenesis models can be developed by differentiating optimal progenitor cells from

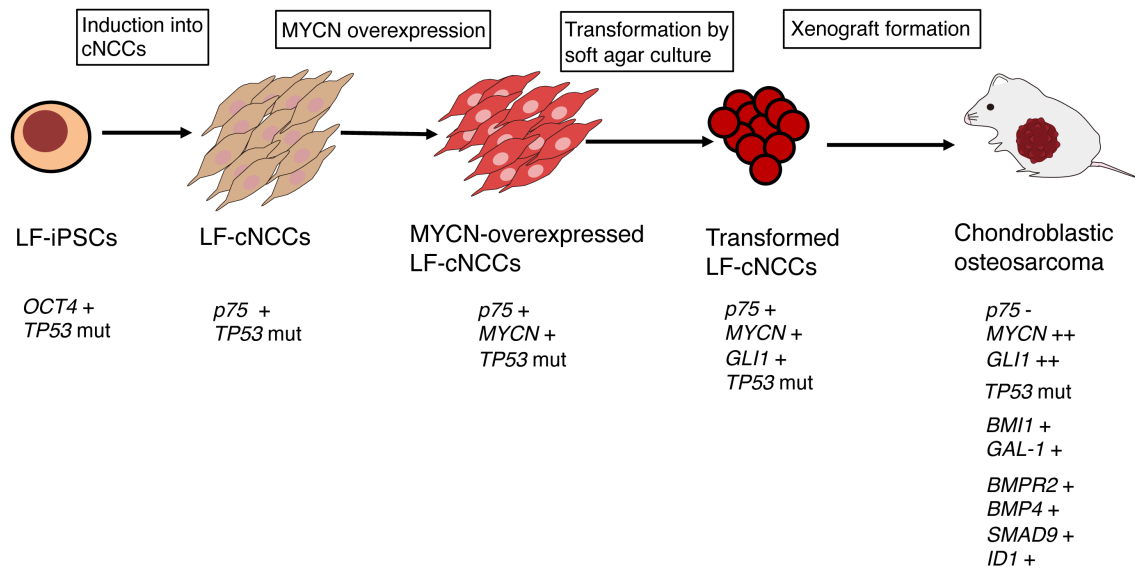


FIGURE 8 Development of a chondroblastic osteosarcoma model from iPSC-based NCCs. Transformed LF cNCCs by MYCN overexpression and soft agar culture generate chondroblastic osteosarcoma with the upregulation of genes involved in osteosarcoma tumorigenesis (*BMI1* and *GAL-1*) and the TGF- β signaling pathway (*BMPR2*, *BMP4*, *SMAD9*, and *ID1*).

hiPSCs and introducing specific gene modifications of oncogenes/TSGs when applying this system. In vitro tumorigenesis models using hiPSCs-derived differentiated cells are an invaluable tool for assessing the contribution of specific genes to the pathogenesis of tumors and screening therapeutic compounds for tumorigenesis models derived from individual patients.

AUTHOR CONTRIBUTIONS

K.M., H.T., and T.K. designed this study; K.M. performed most of the experiments; H.T., Y.E., M.H., T.S., S.S., M.F., J.T., K.O., T.N., and H.K. assisted in some experiments; K.M., T.K., and M.O. wrote the paper.

ACKNOWLEDGMENTS

We thank Editage (www.editage.jp) for English language editing, and Ms. Kimie Nomura for technical assistance.

FUNDING INFORMATION

This study was supported by grants from the Japan Society for the Promotion of Science (JSPS) KAKENHI grant nos. JP 19K16759, JP 19H03625, and JP 22H04922 (AdAMS).

CONFLICT OF INTEREST STATEMENT

Takehiko Kamijo, Miki Ohira, and Junya Toguchida are Editors of Cancer Science. The other authors have no conflict of interest.

ETHICS STATEMENT

The authors declare:

Approval of the research protocol by an Institutional Reviewer Board. The study was approved by the Ethics Committee of the Saitama Cancer Center (approval number 1060) and consent for the use of LF hiPSC and publication of the data was obtained

from the patient. The study was performed in accordance with the Declaration of Helsinki.

Informed Consent. Written informed consent was obtained from all patients.

Registry and the Registration No. of the study/trial: N/A.

Animal Studies. All animals were maintained and used for experiments in accordance with the guidelines of the Institutional Animal Experiments Committee of Saitama Cancer Center.

ORCID

Kyosuke Mukae <https://orcid.org/0000-0001-6411-2990>

Yuki Endo <https://orcid.org/0000-0002-5658-0142>

Miki Ohira <https://orcid.org/0000-0001-9105-1142>

Takehiko Kamijo <https://orcid.org/0000-0003-4798-7546>

REFERENCES

- Komura S, Semi K, Itakura F, et al. An EWS-FLI1-induced osteosarcoma model unveiled a crucial role of impaired osteogenic differentiation on osteosarcoma development. *Stem Cell Rep.* 2016;6(4):592-606. doi:10.1016/j.stemcr.2016.02.009
- Cohen MA, Zhang S, Sengupta S, et al. Formation of human neuroblastoma in mouse-human neural crest chimeras. *Cell Stem Cell.* 2020;26(4):579-592. doi:10.1016/j.stem.2020.02.001
- Fukuta M, Nakai Y, Kirino K, et al. Derivation of mesenchymal stromal cells from pluripotent stem cells through a neural crest lineage using small molecule compounds with defined media. *PLoS One.* 2014;9(12):e112291. doi:10.1371/journal.pone.0112291
- Delaney SP, Julian LM, Stanford WL. The neural crest lineage as a driver of disease heterogeneity in tuberous sclerosis complex and Lymphangioliomyomatosis. *Front Cell Dev Biol.* 2014;2:69. doi:10.3389/fcell.2014.00069
- Donato G, Ivan P, Arcidiacono B, et al. Innate and adaptive immunity linked to recognition of antigens shared by neural crest-derived tumors. *Cancer.* 2020;12(4):840. doi:10.3390/cancers12040840

6. Wu T, Chen G, Tian F, Liu HX. Contribution of cranial neural crest cells to mouse skull development. *Int J Dev Biol*. 2017;61(8-9):495-503. doi:10.1387/ijdb.170051gc
7. Otte J, Dyberg C, Pepich A, Johesen JI. MYCN function in neuroblastoma development. *Front Oncol*. 2020;10:624079. doi:10.3389/fonc.2020.624079
8. Poli V, Fagnocchi L, Fasciani A, et al. MYC-driven epigenetic reprogramming favors the onset of tumorigenesis by inducing a stem cell-like state. *Nat Commun*. 2018;9(1):1-16. doi:10.1038/s41467-018-03264-2
9. Althoff K, Beckers A, Bell E, et al. A Cre-conditional MYCN-driven neuroblastoma mouse model as an improved tool for pre-clinical studies. *Oncogene*. 2015;34(26):3357-3368. doi:10.1038/onc.2014.269
10. Okita K, Matsumura Y, Sato Y, et al. A more efficient method to generate integration-free human iPS cells. *Nat Methods*. 2011;8(5):409-412. doi:10.1038/nmeth.1591
11. Geens L, Robays JV, Geert V, et al. An unusual location of extraosseous Ewing's sarcoma. *Case Rep Oncol*. 2013;6(2):293-302. doi:10.1159/000351836
12. Minas TZ, Surdez D, Javaheri T, et al. Combined experience of six independent laboratories attempting to create an Ewing sarcoma mouse model. *Oncotarget*. 2017;8(21):34141. doi:10.18632/oncotarget.9388
13. Kawane T, Qin X, Jiang Q, et al. Runx2 is required for the proliferation of osteoblast progenitors and induces proliferation by regulating Fgfr2 and Fgfr3. *Sci Rep*. 2018;8(1):1-17. doi:10.1038/s41598-018-31853-0
14. Takahata Y, Hagino H, Kimura A, et al. Smoc1 and Smoc2 regulate bone formation as downstream molecules of Runx2. *Commun Biol*. 2021;4(1):1-11. doi:10.1038/s42003-021-02717-7
15. Lucero CMJ, Vega OA, Osorio MM, et al. The cancer-related transcription factor Runx2 modulates cell proliferation in human osteosarcoma cell lines. *J Cell Physiol*. 2013;228(4):714-723. doi:10.1002/jcp.24218
16. Kleinerman MD. *Current Advances in Osteosarcoma*. Vol 804. Springer International Publishing; 2014.
17. Fang F, VanCleave A, Helmuth R, et al. Targeting the Wnt/ β -catenin pathway in human osteosarcoma cells. *Oncotarget*. 2018;9(95):36780. doi:10.18632/oncotarget.26377
18. Recine F, Bongiovanni A, Riva N, et al. Update on the role of trabectedin in the treatment of intractable soft tissue sarcomas. *Onco Targets Ther*. 2017;10:1155-1164. doi:10.2147/OTT.S127955
19. López-Pousa A, Martín Broto J, Martínez Trufero J, et al. SEOM clinical guideline of management of soft-tissue sarcoma (2016). *Clin Transl Oncol*. 2016;18(12):1213-1220. doi:10.1007/s12094-016-1574-1
20. Naka N, Takenaka S, Araki N, et al. Synovial sarcoma is a stem cell malignancy. *Stem Cells*. 2010;28(7):1119-1131. doi:10.1002/stem.452
21. Spiguel A. *Soft Tissue Sarcomas*. Vol 162. Springer Orthopaedic Oncology; 2014:203-223. doi:10.1007/978-3-319-07323-1_10
22. Li X, Liu R, Shi T, et al. Primary pulmonary malignant fibrous histiocytoma: case report and literature review. *J Thorac Dis*. 2017;9(8):E702. doi:10.21037/jtd.2017.07.59
23. Feng W, Dean DC, Hornicek FJ, et al. Myc is a prognostic biomarker and potential therapeutic target in osteosarcoma. *Ther Adv Med Oncol*. 2020;12:1758835920922055. doi:10.1177/1758835920922055
24. Both J, Krijgsman O, Bras J, et al. Focal chromosomal copy number aberrations identify CMTM8 and GPR177 as new candidate driver genes in osteosarcoma. *PLoS One*. 2014;9(12):e115835. doi:10.1371/journal.pone.0115835
25. Smida J, Xu H, Zhang Y, et al. Genome-wide analysis of somatic copy number alterations and chromosomal breakages in osteosarcoma. *Int J Cancer*. 2017;141(4):816-828. doi:10.1002/ijc.30778
26. Sato M, Larsen JE, Lee W, et al. Human lung epithelial cells progressed to malignancy through specific oncogenic manipulations. *Mol Cancer Res*. 2013;11(6):638-650. doi:10.1158/1541-7786.MCR-12-0634-T
27. Terada Y, Jo N, Arakawa Y, et al. Human pluripotent stem cell-derived tumor model uncovers the embryonic stem cell signature as a key driver in atypical teratoid/rhabdoid tumor. *Cell Rep*. 2019;26(10):2608-2621. doi:10.1016/j.celrep.2019.02.009
28. Xue Y, Fu Y, Zhao F, et al. Frondoside a inhibits an MYC-driven medulloblastoma model derived from human-induced pluripotent stem cells. *Mol Cancer Ther*. 2021;20(6):1199-1209. doi:10.1158/1535-7163.MCT-20-0603
29. Lee DF, Su J, Kim HS, et al. Modeling familial cancer with induced pluripotent stem cells. *Cell*. 2015;161(2):240-254. doi:10.1016/j.cell.2015.02.045
30. Mutsaers AJ, Walkley CR. Cells of origin in osteosarcoma: mesenchymal stem cells or osteoblast committed cells? *Bone*. 2014;62:56-63. doi:10.1016/j.bone.2014.02.003
31. Pompetti F, Rizzo P, Simon RM, et al. Oncogene alterations in primary, recurrent, and metastatic human bone tumors. *J Cell Biochem*. 1996;63(1):37-50. doi:10.1158/1535-7163.MCT-20-0603
32. Wu Z, Min L, Chen D, et al. Overexpression of BMI-1 promotes cell growth and resistance to cisplatin treatment in osteosarcoma. *PLoS One*. 2011;6(2):e14648. doi:10.1371/journal.pone.0014648
33. Gomez-Brouchet A, Mourcin F, Gourraud PA, et al. Galectin-1 is a powerful marker to distinguish chondroblastic osteosarcoma and conventional chondrosarcoma. *Hum Pathol*. 2010;41(9):1220-1230. doi:10.1016/j.humpath.2009.10.028
34. Salas S, de Pinieux G, Gomez-Brouchet A, et al. Ezrin immunohistochemical expression in cartilaginous tumours: a useful tool for differential diagnosis between chondroblastic osteosarcoma and chondrosarcoma. *Virchows Arch*. 2009;454(1):81-87. doi:10.1007/s00428-008-0692-8
35. Robles AI, Jen J, Harris CC. Clinical outcomes of TP53 mutations in cancers. *Cold Spring Harb Perspect Med*. 2016;6(9):a026294. doi:10.1101/cshperspect.a026294
36. Kuijjer ML, Namløs HM, Hauben EI, et al. mRNA expression profiles of primary high-grade central osteosarcoma are preserved in cell lines and xenografts. *BMC Med Genomics*. 2011;4(1):1-12. doi:10.1186/1755-8794-4-66
37. Zhou Y, Yang D, Yang Q, et al. Single-cell RNA landscape of intratumoral heterogeneity and immunosuppressive microenvironment in advanced osteosarcoma. *Nat Commun*. 2020;11(1):1-17. doi:10.1038/s41467-020-20059-6
38. Katoh Y, Katoh M. Integrative genomic analyses on GLI1: positive regulation of GLI1 by hedgehog-GLI, TGF β -Smads, and RTK-PI3K-AKT signals, and negative regulation of GLI1 by notch-CSL-HES/HEY, and GPCR-Gs-PKA signals. *Int J Oncol*. 2009;35(1):187-192. doi:10.3892/ijo.00000328
39. Takano Y, Kato Y, Masuda M, Ohshima Y, Okayasu I. Cyclin D2, but not cyclin D1, overexpression closely correlates with gastric cancer progression and prognosis. *J Pathol*. 1999;189(2):194-200. doi:10.1002/(SICI)1096-9896(199910)189:2%3C194::AID-PATH426%3E3.0.CO;2-P
40. Doush Y, Surani AA, Navarro-Corcuera A, McArdle S, Billett EE, Montiel-Duarte C. SP1 and RAR α regulate AGAP2 expression in cancer. *Sci Rep*. 2019;9:1-12. doi:10.1038/s41598-018-36888-x
41. Shu X, Li X, Xiang X, Wang Q, Wu Q. METTL21B is a prognostic biomarker and potential therapeutic target in low-grade gliomas. *Aging*. 2021;13(16):20661-20683. doi:10.18632/aging.203454
42. Iwata S, Tatsumi Y, Yonemoto T, et al. CDK4 overexpression is a predictive biomarker for resistance to conventional chemotherapy in patients with osteosarcoma. *Oncol Rep*. 2021;46(1):1-11. doi:10.3892/or.2021.8086

43. Zhang J, Liu S, Li Q, et al. The deubiquitylase USP2 maintains ErbB2 abundance via counteracting endocytic degradation and represents a therapeutic target in ErbB2-positive breast cancer. *Cell Death Differ.* 2020;27(9):2710-2725. doi:[10.1038/s41418-020-0538-8](https://doi.org/10.1038/s41418-020-0538-8)
44. Wang W, Yan T, Guo W, et al. Constitutive GLI1 expression in chondrosarcoma is regulated by major vault protein via mTOR/S6K1 signaling cascade. *Cell Death Differ.* 2021;28(7):2221-2237. doi:[10.1038/s41418-021-00749-4](https://doi.org/10.1038/s41418-021-00749-4)
45. Fry DW, Harvey PF, Keller PR, et al. Specific inhibition of cyclin-dependent kinase 4/6 by PD 0332991 and associated anti-tumor activity in human tumor xenografts. *Mol Cancer Ther.* 2004;3(11):1427-1438. doi:[10.1158/1535-7163.1427.3.11](https://doi.org/10.1158/1535-7163.1427.3.11)

SUPPORTING INFORMATION

Additional supporting information can be found online in the Supporting Information section at the end of this article.

How to cite this article: Mukae K, Takenobu H, Endo Y, et al. Development of an osteosarcoma model with MYCN amplification and TP53 mutation in hiPS cell-derived neural crest cells. *Cancer Sci.* 2023;114:1898-1911. doi:[10.1111/cas.15730](https://doi.org/10.1111/cas.15730)